

PAPER • OPEN ACCESS

## Programmable droplet actuating platform using liquid dielectrophoresis

To cite this article: Iman Frozanpoor *et al* 2021 *J. Micromech. Microeng.* **31** 055014

View the [article online](#) for updates and enhancements.

You may also like

- [Electrical actuation of electrically conducting and insulating droplets using ac and dc voltages](#)  
N Kumari, V Bahadur and S V Garimella
- [Nanopore-based active oil droplet filtration under negative DC dielectrophoresis for oily wastewater treatment](#)  
Qinlong Ren, Zexiao Wang, Ning Liu et al.
- [Frequency-controlled dielectrophoresis-driven wetting of nematic liquid crystals](#)  
Carl V Brown, Akshay S Bhadwal, Andrew M J Edwards et al.

# Programmable droplet actuating platform using liquid dielectrophoresis

Iman Frozanpoor<sup>1,\*</sup> , Michael Cooke<sup>1</sup>, Zoltan Racz<sup>1</sup>, Ian Bossons<sup>2</sup>, Vibin Ambukan<sup>2</sup>, David Wood<sup>3</sup>, Andrew Gallant<sup>1</sup> and Claudio Balocco<sup>1</sup>

<sup>1</sup> Department of Engineering, Durham University, South Rd, Durham DH1 3LE, United Kingdom

<sup>2</sup> Jaguar Land Rover Limited, National Automotive Innovation Centre, Coventry CV4 7AL, United Kingdom

<sup>3</sup> Department of Mathematics, Physics and Electrical Engineering, Northumbria University, Newcastle-upon-Tyne NE1 8ST, United Kingdom

E-mail: [Iman.frozanpoor@durham.ac.uk](mailto:Iman.frozanpoor@durham.ac.uk)

Received 5 December 2020, revised 1 March 2021

Accepted for publication 18 March 2021

Published 20 April 2021



CrossMark

## Abstract

Droplet motion has been a long-standing interest in microfluidics as it is often limited by the high operating voltages, which hampers the development of consumer applications. Forces generated by liquid dielectrophoresis (L-DEP) can enhance surface wetting, without requiring chemical modification or surface texturing. This work presents a droplet actuating platform to control the wetting behaviour of water droplets using L-DEP. The exploitation of high electric fields at the droplet solid–liquid interface reduced the operating voltages. The operating voltage can be further reduced, to as low as 30 V, by introducing a lubricant layer to minimise the droplet contact angle hysteresis, thus requiring a smaller L-DEP bulk force. The outcomes of this study will provide a new pathway for developing energy-efficient and reliable droplet actuating platforms to clean a variety of surfaces. A particular interest will be the application of this system in the automobile sector, for instance, to clean headlamps, sensors, cameras, door mirrors, front side glass, and rear screen.

Supplementary material for this article is available [online](#)

Keywords: liquid dielectrophoresis, microfluidics, microfabrication, droplet actuation, electric field

(Some figures may appear in colour only in the online journal)

## 1. Introduction

The control of sessile droplets on a planar surface has extensive applications in both industrial and domestic environments, extending from surface cleaning platforms to medical and pharmaceutical analysis. The two most conventional methods for the electrical control of droplets are electrowetting and

dielectrowetting [1, 2]. Electrowetting behaviour is predominantly investigated with a range of practical constraints [3, 4]. For instance, the contact angle saturation phenomenon is a limiting factor, and it is only compatible with conductive liquids [5]. Furthermore, the droplet manipulations are typically performed using a sandwich-structure with a covering top-plate [6]. Dielectrowetting, on the other hand, has been gaining considerable attention for overcoming the limitations of electrowetting [7]. Dielectrowetting is based on liquid dielectrophoresis (L-DEP), which is a bulk force generated when a non-uniform electric field interacts with the electric dipoles within a liquid [8]. The spreading of droplets into a thin film was initially performed to show that dielectrowetting can overcome the contact angle saturation limitation of electrowetting [9].

\* Author to whom any correspondence should be addressed.



Original content from this work may be used under the terms of the [Creative Commons Attribution 4.0 licence](#). Any further distribution of this work must maintain attribution to the author(s) and the title of the work, journal citation and DOI.

This critical study also established the foundation of interface-localised L-DEP, and following it, the L-DEP effect at the solid–liquid interface of a droplet was thoroughly investigated to verify a relationship between the change of contact angle and applied voltage [10]. The behaviour of droplet actuation using L-DEP has attracted a great deal of research interest for diverse applications, notably in the fields of optofluidics and lab-on-a-chip microfluidic devices [11, 12]. The actuation of deionised (DI) water and other dielectric solutions in a microfluidic system has also been demonstrated using L-DEP forces, enabling the further development of smaller micro-total analysis systems [13–15]. The manipulation of discrete droplets using dielectrowetting was recently presented using interdigitated electrodes (IDE's) to actuate dielectric droplets [16]. For the first time, a device based on L-DEP was tested capable of splitting and transporting dielectric liquid droplets in a discrete manner operating in excess of 340 V. The actuation of sessile droplets using L-DEP can be explained through asymmetric electrostatic forces changing the contact angle on one side of the droplet, thus causing motion. The study also highlights the critical frequency for DI water and propylene carbonate that guarantees a dielectric response consistent with expectations of operating above a cross-over frequency.

Our study presents a programmable platform that is unlike electrowetting-based designs with a specific focus on the large-scale actuation of droplets with a variable volume using an iterative switching method.

## 2. Material and methods

### 2.1. Design and fabrication

The conceptual design of a device with four separate layers is presented in figure 1(a). Standard photolithography was used to pattern the electrodes on the glass substrate (see figure 1(b)). 70 nm of aluminium was deposited by E-beam evaporation, followed by a lift-off process. The objective of the sample preparation was based around minimising the thickness of the covering insulating layers to maximise the device performance. A common photosensitive epoxy resin (SU-8 2000.5), with a thickness of 500 nm was used as a dielectric material on the electrodes to chemically, electrically and mechanically protect them during testing. The thickness of this layer was measured using a profilometer and was found to be 500 nm and up to 600 nm. The layer was functionalised with a hydrophobic self-assembled monolayer (SAM), octadecyltrichlorosilane (OTS), to enhance its hydrophobicity. The observed contact angle of the OTS surface was found to be  $110^\circ (\pm 3^\circ)$ , confirming the hydrophobic enhancement of the SU-8 layer while minimising the overall thickness of the covering top layers (see figure 1(c)).

### 2.2. Experimental setup

A modular electronic control system with a relay module was custom-designed, allowing control of individual high-speed reed relays by simple commands from a host PC. The general

overview of the electronic-modules is shown in figure 2. Please refer to the supporting document for more details.

A testing probe station with up to 36 contacts was made to facilitate the electrical connection between the device and the electronic-module. The testing stage was designed so that both the top view as well as the side view of the droplets can be video recorded using a vertically mounted camera. MATLAB software was used to connect, control and store picture and video files. Mbed-OS provided the Mbed (C/C++) software platform to generate algorithms for controlling the switching patterns of the electrodes.

## 3. Results and discussions

### 3.1. Spreading of droplets

Here, we report on the low-voltage L-DEP actuation of droplets. The reduction in the operating voltage stems from the higher electric-field gradient produced by scaling down the electrode dimensions to the micron scale [10, 17]. The effect of change in contact angle was limited in previous dielectrowetting studies by the fixed thickness of the hydrophobic and insulating covering layers (a few micrometres) to withstand higher operating voltages to achieve a complete film formation (250 V or more).

The smaller electrodes produce a lower penetration depth into the liquid, hence requiring a thinner insulating covering layer. Dielectric layers thinner than 500 nm were avoided because of issues related to dielectric breakdown and lower operational lifespan. Additionally, the thickness of the OTS layer is on the nanoscopic scale. Variations of SAMs and SU-8 have already been thoroughly studied and used in many electronic applications [18–20]. However, the SAM functionalised SU-8 dielectric layer is uncommon for a dielectrowetting study. Furthermore, the OTS coating technique is cost-effective, scalable, and widely available.

COMSOL Multiphysics was used to numerically simulate the relationship between the electrode gap distance and the electric field (see figure 3(a)). The study emphasises the importance of reducing the electrode gap distance and the covering dielectric and hydrophobic top layers to produce a sufficiently high enough DEP force at the solid–liquid interface for a fixed operating voltage. This optimisation mechanism was based on the previous studies of L-DEP and DEP [10, 21]. The DEP force is defined by the field factor, and the electrode geometries play a crucial factor during the experimental design. Notably, deeper penetration of the electric field into the liquid generates a larger force, but the L-DEP effect is most critical at the local liquid–solid interface. In addition, testing thicker insulating layers reduced the device performance.

To better understand the droplet driving behaviour, a series of single electrodes with different gap geometries were also tested (see figures 3(b) and (c)). The alternating current voltages in the experiments denote root-mean-square, and DC signals are avoided because of lower electric field penetration into the droplets. The experiment was conducted in ambient conditions, and the obtained results confirm that a change of contact angle similar to those reported in previous studies is

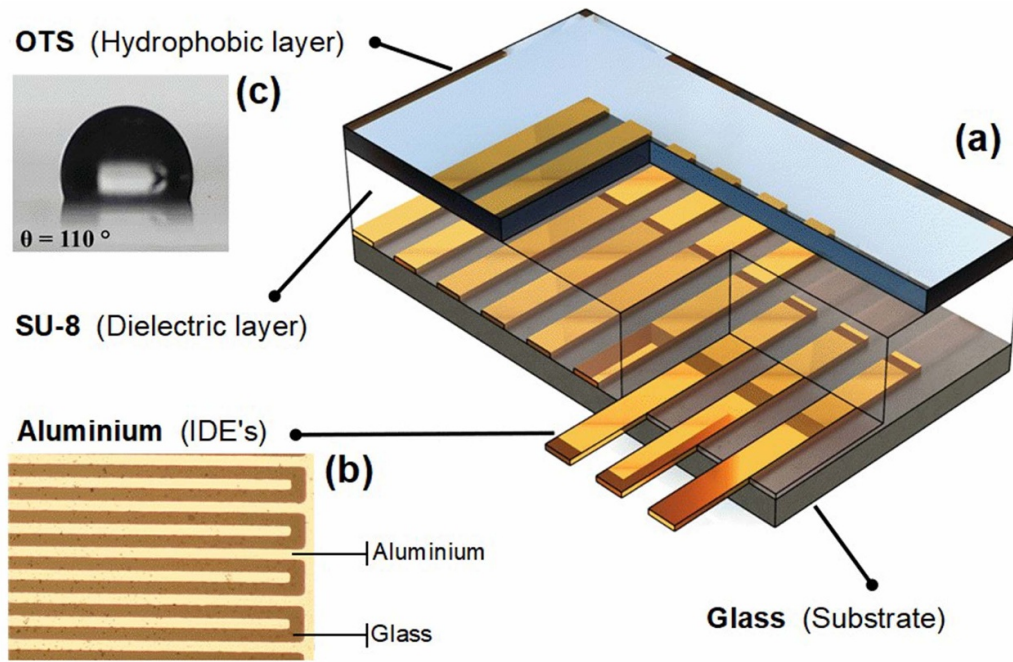


**Figure 1.** (a) 3D schematic of a typical device with four separate layers: glass, aluminium, SU-8 and OTS. (b) Top view optical microscope image of an electrode pad. Note that the image is showing part of the electrode pads. (c) Side view image of a water droplet on an OTS surface.

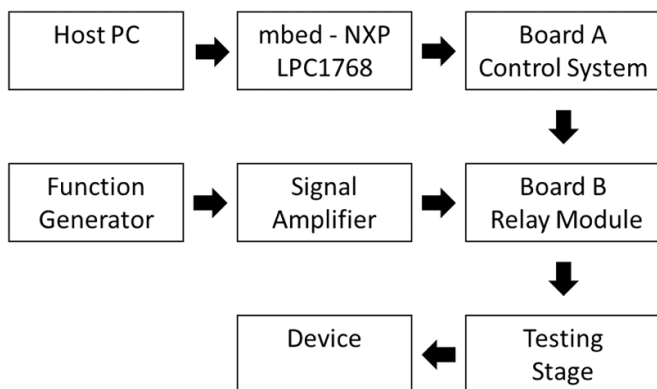


**Figure 2.** The electronic-modules for the programmable platform. The host PC is connected to a microcontroller to control up to 128 output signals from the control system (board A) to the relay module (board B). Function generator facilitated AC waveforms over a wide range of frequencies and amplified with a signal amplifier. The high voltage signals were connected to the device via the testing stage with an array of pogo pins.

still possible when smaller electrode gaps with an appropriate insulating thickness are used. The L-DEP bulk force is frequency dependent, with an optimum crossover frequency of 20 kHz and 40 kHz for propylene carbonate and DI water, respectively. The dielectrophoretic response is related to the magnitude of the electric field, and the effect is only visible at higher frequencies (30–50 kHz), for electrodes with a 20  $\mu\text{m}$  gap distance (see figure S3). Additionally, the experimental results confirm that the cosine of contact angle is proportional to the applied voltage squared, similar to electrowetting (see figure S4).

### 3.2. Droplet actuation

From a technological and commercial perspective, lower operating voltages are desirable to avoid complex electronics, electromagnetic compatibility, and safety concerns. The droplet transportation mechanism with the three actuation steps are presented in figures 4(a) and (b) shows 36 IDE's, used to actuate DI water droplets. Linear actuation was achieved at 105 V, with a measured average speed of 20  $\text{mm s}^{-1}$ . Higher operating voltages reduced the average device lifespan and in some cases, resulted in a dielectric breakdown for thinner dielectric layers. On the other hand, using thicker insulating layers significantly reduced the bulk DEP force, leading to smaller changes in the contact angle. Thus far, we have shown that electric fields can manipulate water droplets to wet a solid surface using low-voltages, and potential further refinement is feasible. Even lower operating voltages can be used when the top layer is coated with a lubricant layer [22]. The surface treatment reduces the contact angle hysteresis associated with the pinning forces at the droplet contact line. Indeed, previous work on electrowetting reported that the contact angle hysteresis associated with the pinning effect could be minimised to produce a reversible spreading of droplets using a thin oil layer [23, 24]. Note that the surface treatment remained functional without any noticeable change within the testing period (at least 2–3 months).

The oil treatment is an alternative method to enhance the hydrophobicity of the surface to minimise the contact angle hysteresis, and similar results may also be obtained using an enhanced OTS surface with superhydrophobic wetting properties [19]. The actuation of DI water droplets was achieved at a voltage as low as 30 V when a layer of mineral oil with

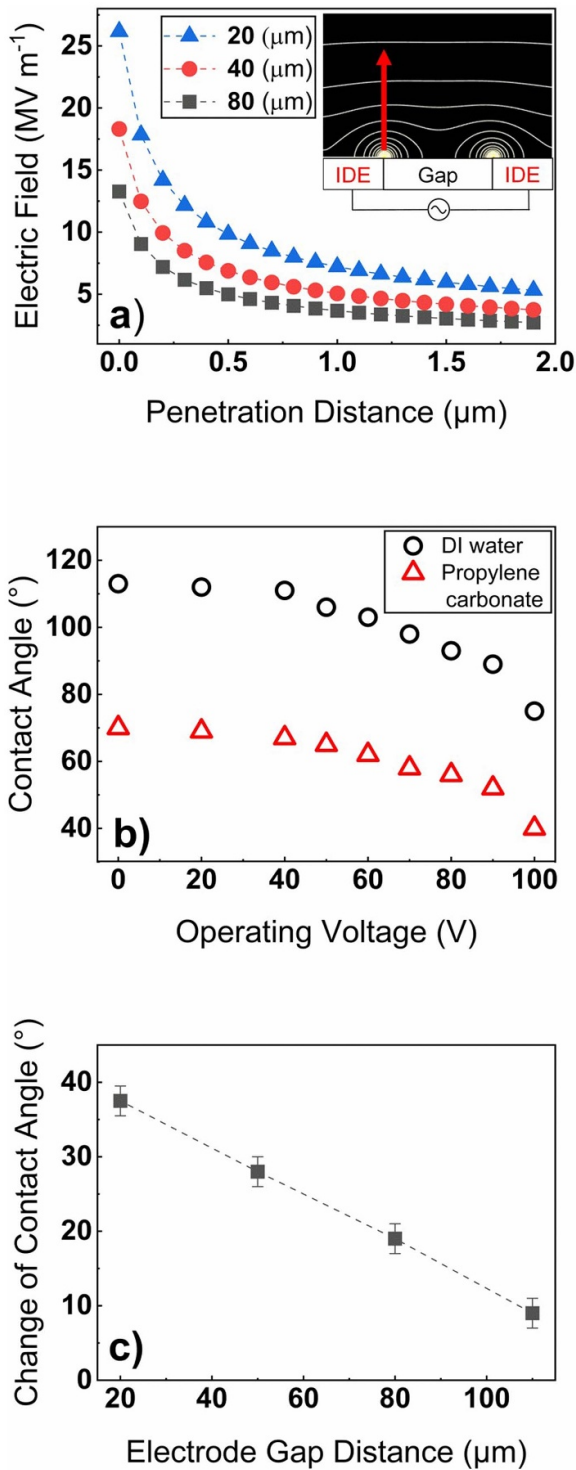


**Figure 3.** Experimental and simulation data. The electric signals here are presented in root mean square (RMS) voltage. (a) COMSOL simulation models showing the decay of the electric field at a fixed voltage of 100 V. (Insert) The sub-figure in here represents the electric field distribution between two electrode pads and the red arrow shows the penetration depth in the medium. (b) Change of contact angle for DI water (sine-wave signal with a frequency of 40 kHz), and propylene carbonate droplets (sine-wave signal with a frequency of 20 kHz), at different operating voltages with an electrode gap distance of 20  $\mu\text{m}$ . (c) The change of contact angle for a DI water droplets with 100 V of operating voltage (sine-wave signal with a frequency of 40 kHz) for different electrode gap geometries.

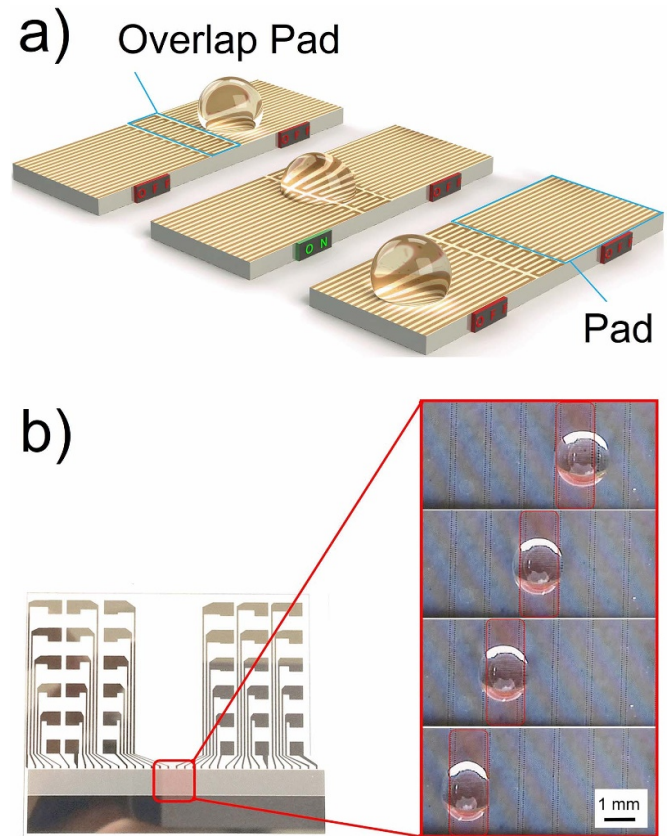


**Figure 4.** The Linear actuation of droplets. (a) Three actuation steps of a 3D water droplet model on a platform: the electrodes are activated (ON) when an AC voltage source is connected to the signal and ground terminals. There is an overlap-pad for a smooth droplet transition of every switching step. (b) Top view of the device with 36 electrode sets (6  $\times$  1 mm) to actuate DI water droplet using 95 V at 40 kHz. Here the activated electrodes are represented with a rectangular box with an average actuation speed of 9  $\text{mm s}^{-1}$ .

an average thickness of 100  $\mu\text{m}$  covered the device. The thickness of this layer was regulated by controlling the volume of the oil injected over a confined area and then spin-coated to aid uniformity. The surface treatment was possible since the OTS layer was oleophilic. The actuation speed was severely reduced due to the drop in the electrostatic energy per unit contact area, which is determined by the applied voltage and penetration of the electric fields in the water layer [10, 21]. Nevertheless, faster switching speeds with lower operating voltages may still be possible by further reducing the thickness of the lubricant layer to generate higher forces. The lubricant treatment has limited applications, predominantly in microfluidics. In contrast, the actuation of droplets at higher voltages (up to 100 V) on a plain OTS surface is suitable for cleaning applications, i.e. to clean cameras and sensors.

### 3.3. Iterative fractal approach

The manipulation of discrete droplets has been validated in microfluidic systems using a droplet sensing method within a feedback control loop. Such as, vision systems, fluorescence

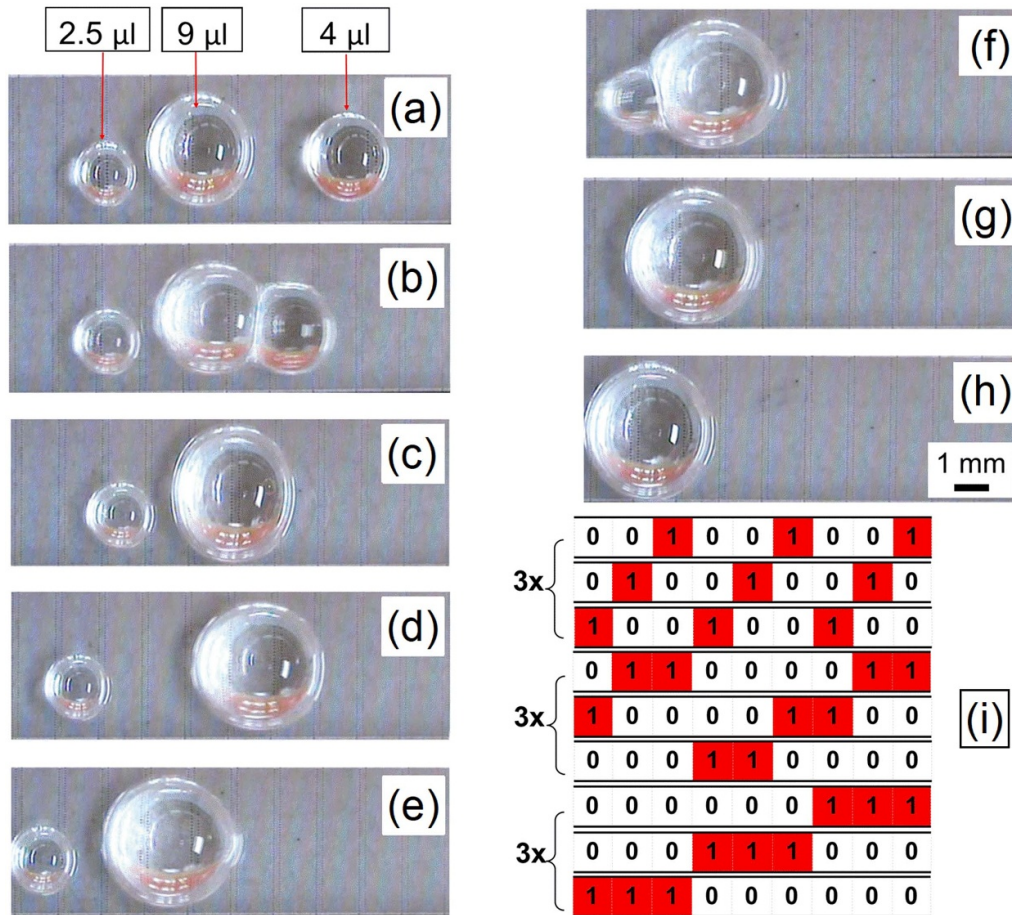


**Figure 5.** Actuation of droplets using an iterative approach. (a)–(h) Actuation of three DI water droplets with different volumes (2.5, 4 and 9 μl) in a single test using the iterative algorithm. The actuation is carried out on a thin lubricant layer using 85 V with a signal frequency of 40 kHz. (i) The algorithm used to transport different volumes of water. The cycles are repeated three times to ensure a complete transition of the droplets to the left side of the device for disposal. This concept can be applied to any number of electrodes on a large surface.

spectroscopy, capacitive sensing, and impedance measurements have all been demonstrated [25–28]. However, these methods are not suitable for a large-scale droplet actuation, i.e. in self-cleaning surfaces due to higher costs, design parameters and complexity. In our approach, an improved design is proposed based on an iterative approach to produce droplet actuation of varying volume without using any active feedback control system. Microscale electrodes can be iteratively combined to effectively realised larger arrays capable of driving larger droplets (see figure 5(i)). The iterative code for actuating droplets with varying volumes is based on the process of recursion (Please refer to the supplementary material (available online at [stacks.iop.org/JMM/31/055014/mmedia](https://stacks.iop.org/JMM/31/055014/mmedia)) for more detail).

The iteration time between each actuation was set by the spreading time of a single droplet, which was approximately 100 ms in our system, with an additional delay (100 ms) to allow precise monitoring of the droplets during the operation [29]. The iterative cycles were applied to a set of electrodes to verify the suitability of the hardware and software for actuating DI water droplets with different volumes (2.5–9 μl), and

the results are summarised in figures 5(a)–(h). The actuation behaviour is directed towards a cleaning application, and it resembles a scrubbing like motion, while at the same time eventually transporting the droplets in one direction for disposal.

The initial steps in the iterative actuation use individual IDE’s to move smaller droplets. However, after 1.5 s, the newly formed larger droplet covers a surface area of more than three IDE’s (see figure 5(c)), and as a consequence, the actuation towards the left side of the device is delayed until a full set of iterations is repeated multiple times. The actuation process of a droplet moving from one electrode to another is only possible when the droplet moves to an area over an IDE which is due to be active. Otherwise, it will move back to the previous electrode for the next set of iterations. Furthermore, depending on the application, the back-and-forth motion may be desirable as it can be used to remove impurities from the surface. Alternatively, a direct linear actuation, which avoids the back and forth motion can be realised using a longer activation time, or a device with a higher electrode resolution.

## 4. Conclusions

In recent years, the droplet motion by electric means has been gaining more attention than other methods such as acoustic, magnetic, pneumatic, and thermal actuation. This is because of the excellent response time, device lifetime, and accuracy of the actuation. However, the technology is limited by the dependence on the droplet size, high fabrication, and experimental setup costs [30]. We verify that the actuation of droplets with varying volume is possible without the need for any active feedback control system. Moreover, the introduction of the iterative switching method is a compelling simple addition that reduces the experimental setup costs. Also, the SAM functionalised SU-8 dielectric layers is a simple and cost-efficient technique to improve the device performance.

The open surface structure in here has advantages compared to the sandwich-structure, including easy droplet access with the external device. However, there also exists a critical limitation that the actuating force is substantially reduced, requiring higher operating voltages. Hence, lowering the voltages for L-DEP droplet actuation expands the application of this technology. Furthermore, for a particular application, the electrodes can be fabricated using indium tin oxide electrodes, which is a widely used transparent conductor with excellent electrical and optical properties (see figure S1). This allows the scrubbing motion presented in this work to remove debris from the surface of a sensor or solar panel.

The L-DEP and electrowetting dominate the microfluidics in the high and low-frequency limits, respectively. Hence, the generated electric fields can penetrate mild ionic solutions (such as rainwater) when they are applied with a sufficiently high frequency [31, 32]. As previously discussed, both of the actuation methods have their pros and cons. This is notably evident for the electrowetting actuation of conductive droplets using lower signal frequencies. There are reported speeds of up to  $70 \text{ mm s}^{-1}$  (100 V at 67 Hz), using large electrode pads with a polished surface treatment [33]. Furthermore, the use of large electrode pads that generate a strong double layer effect is incompatible with the iterative approach demonstrated here that addresses the droplet volume limitation. The future focus of L-DEP droplet actuation should be to obtain comparable performance employing similar surface treatments. This is particularly interesting as the polished surface treatment generated higher electric field values near the liquid–solid interface.

The operational capability to manipulate a range of different liquids using electrowetting and dielectrowetting expands the application of the iterative method to similar droplet actuation concepts [14]. We can thus expect in the next decade to witness the utilisation of programmable droplet actuating platforms for a range of different products, i.e. even to tackle the problem of surface contamination in cars [34].

## Data availability statement

All data that support the findings of this study are included within the article (and any supplementary files).

## Acknowledgments

The authors would like to thank Gary Wells and Jidong Jin for helpful discussions, and Chris Pearson, Neil Clarey and Ian Hutchinson for technical assistance. We are thankful for the financial support provided by Jaguar Land Rover (JLR) and the Engineering and Physical Sciences Research Council (EPSRC), U.K., through the Industrial Case Award EP/P510476/1.

## ORCID iD

Iman Frozanpoor  <https://orcid.org/0000-0002-2754-9867>

## References

- [1] Edwards A M J, Brown C V, Newton M I and McHale G 2018 Dielectrowetting: the past, present and future *Curr. Opin. Colloid Interface Sci.* **36** 28–36
- [2] Nelson W C and Kim C-J C-J 2012 Droplet actuation by electrowetting-on-dielectric (EWOD): a review *J. Adhes. Sci. Technol.* **26** 1747–71
- [3] Zhao Y-P and Wang Y 2013 Fundamentals and applications of electrowetting *Rev. Adhes. Adhes.* **1** 114–74
- [4] Kedzierski J and Holihan E 2018 Linear and rotational microhydraulic actuators driven by electrowetting *Sci. Robot.* **3** eaat5643
- [5] Li X et al 2016 Decreasing the saturated contact angle in electrowetting-on-dielectrics by controlling the charge trapping at liquid–solid interfaces *Adv. Funct. Mater.* **26** 2994–3002
- [6] Kojima T, Lin C-C, Takayama S and Fan S-K 2019 Determination of aqueous two-phase system binodals and tie-lines by electrowetting-on-dielectric droplet manipulation *Chem. Bio. Chem.* **20** 270–5
- [7] Quinn A, Sedev R and Ralston J 2005 Contact angle saturation in electrowetting *J. Phys. Chem. B* **109** 6268–75
- [8] Pohl H A 1978 *Dielectrophoresis: The Behavior of Neutral Matter in Nonuniform Electric Fields* (Cambridge: Cambridge University Press)
- [9] Brown C V, Wells G G, Newton M I and McHale G 2009 Voltage-programmable liquid optical interface *Nat. Photon.* **3** 403
- [10] McHale G, Brown C V, Newton M I, Wells G G and Sampara N 2011 Dielectrowetting driven spreading of droplets *Phys. Rev. Lett.* **107** 186101
- [11] Xu S, Ren H and Wu S-T 2013 Dielectrophoretically tunable optofluidic devices *J. Phys. D: Appl. Phys.* **46** 483001
- [12] Geng H and Cho S K 2017 Dielectrowetting for digital microfluidics: principle and application. A critical review *Rev. Adhes. Adhes.* **5** 268–302
- [13] Washizu M 1998 Electrostatic actuation of liquid droplets for micro-reactor applications *IEEE Trans. Ind. Appl.* **34** 732–7
- [14] Geng H and Cho S K 2019 Antifouling digital microfluidics using lubricant infused porous film *Lab Chip* **19** 2275–83
- [15] Ren H, Xu S and Wu S-T 2013 Liquid crystal pump *Lab Chip* **13** 100–5
- [16] Geng H, Feng J, Stabryla L M and Cho S K 2017 Dielectrowetting manipulation for digital microfluidics: creating, transporting, splitting, and merging of droplets *Lab Chip* **17** 1060–8
- [17] Jones T B 2001 Liquid dielectrophoresis on the microscale *J. Electrostat.* **51–52** 290–9
- [18] Gupta S K et al 2009 Self-assembled and electrochemically deposited mono/multilayers for molecular electronics applications *Appl. Surf. Sci.* **256** 407–13

- [19] Kumar V and Sharma N N 2015 Synthesis of hydrophilic to superhydrophobic SU8 surfaces *J. Appl. Polym. Sci.* **132** 41934
- [20] Salomon S, Leichlé T and Nicu L 2011 A dielectrophoretic continuous flow sorter using integrated microelectrodes coupled to a channel constriction *Electrophoresis* **32** 1508–14
- [21] Pethig R 2017 *Dielectrophoresis: Theory, Methodology, and Biological Applications* 1st edn (New York: Wiley)
- [22] Wong T-S et al 2011 Bioinspired self-repairing slippery surfaces with pressure-stable omniphobicity *Nature* **477** 443
- [23] Brabcova Z, McHale G, Wells G G, Brown C V and Newton M I 2017 Electric field induced reversible spreading of droplets into films on lubricant impregnated surfaces *Appl. Phys. Lett.* **110** 121603
- [24] Hao C et al 2014 Electrowetting on liquid-infused film (EWOLF): complete reversibility and controlled droplet oscillation suppression for fast optical imaging *Sci. Rep.* **4** 6846
- [25] Armani M, Chaudhary S, Probst R, Walker S and Shapiro B 2005 Control of microfluidic systems: two examples, results, and challenges *Int. J. Robust Nonlinear* **15** 785–803
- [26] Schwartz J A, Vykoukal J V and Gascoyne P R C 2004 Droplet-based chemistry on a programmable micro-chip *Lab Chip* **4** 11–7
- [27] Isgor P K, Marcali M, Keser M and Elbuken C 2015 Microfluidic droplet content detection using integrated capacitive sensors *Sensors Actuators B* **210** 669–75
- [28] Sadeghi S et al 2012 On chip droplet characterization: a practical, high-sensitivity measurement of droplet impedance in digital microfluidics *Anal. Chem.* **84** 1915–23
- [29] McHale G, Brown C V and Sampara N 2013 Voltage-induced spreading and superspreading of liquids *Nat. Commun.* **4** 1605
- [30] Xi H-D et al 2017 Active droplet sorting in microfluidics: a review *Lab Chip* **17** 751–71
- [31] Jones T B, Fowler J D, Chang Y S and Kim C-J 2003 Frequency-based relationship of electrowetting and dielectrophoretic liquid microactuation *Langmuir* **19** 7646–51
- [32] Jones T B, Wang K-L and Yao D-J 2004 Frequency-dependent electromechanics of aqueous liquids: electrowetting and dielectrophoresis *Langmuir* **20** 2813–8
- [33] Shirinkami H, Kim J, Lee C, Kim H C and Chun H 2017 Improvement of droplet speed and stability in electrowetting on dielectric devices by surface polishing *Biochip J.* **11** 316–21
- [34] Gaylard A P, Kirwan K and Lockerby D A 2017 Surface contamination of cars: a review *Proc. Inst. Mech. Eng. D* **231** 1160–76